IEEE Access
Multidisciplinary | Rapid Review | Open Access Journal

Received November 3, 2020, accepted November 26, 2020, date of publication December 1, 2020,
date of current version December 11, 2020.

Digital Object Identifier 10.1109/ACCESS.2020.3041533

A Novel Self-Adaptive Wind Speed Prediction Model Considering Atmospheric Motion and Fractal Feature

JI JIN[1], BIN WANG[1], MIN YU[2], JIANG LIU[1], AND WENBO WANG[2]
[1]School of Information Science and Engineering, Wuhan University of Science and Technology, Wuhan 430081, China
[2]College of Science, Wuhan University of Science and Technology, Wuhan 430065, China

Corresponding author: Min Yu (yufeng3378@163.com)

This work was supported in part by the National Natural Science Foundation of China under Grant 51877161 and Grant 61671338, in part by the Coordination and Innovation Centre of Process Control and Advanced Equipment Manufacturing Project of Hubei province, China under Grant HX2016A1005, and in part by the Scientific Research Foundation of Hubei Education Department of China under Grant B2018006.

ABSTRACT Many of the previous investigations predicted wind speed by directly using wind speed data, which rarely considered physical characteristics of wind speed and was difficult to improve prediction accuracy further. Therefore, a novel self-adaptive wind speed prediction model considering atmospheric motion and fractal feature is developed in this paper. Lorenz-Stenflo (LS) equation is employed to describe the disturbances and chaos effect caused by atmospheric motion on wind speed. One-dimension LS motion series obtained by LS equation is adopted to improve the decomposition effect of wind speed by ensemble empirical mode decomposition (EEMD). The fractal feature of wind speed series is primitively adopted to determine the key parameter in LS equation. Then back propagation (BP) neural network model optimized by genetic algorithm (GA), as a fundamental prediction model, is used for prediction. Eight groups of wind speed series on different time scales from two wind farms are tested and evaluated. The proposed model effectively overcomes the disturbances of atmospheric motion and achieves promising prediction accuracy. Meanwhile, the criterion based on fractal feature ensures accurate selection of the key parameter in atmospheric motion equation according to different features of sampled wind data.

INDEX TERMS Wind speed prediction, atmospheric motion, LS equation, EEMD, fractal feature.

I. INTRODUCTION

With the depletion of traditional fossil fuels and increasingly serious environmental problems, wind energy has been highly valued by countries in the world [1], [2]. According to the data released by the Global Wind Energy Council (GWEC), the cumulative installed capacity of the global wind power market exceeded 500GW [3]. However, wind energy is characterized by randomness and volatility etc. Large-scale wind power integration brings great volatility to grid and hampers safe and stable operation of the grid [4]. Accurate prediction to wind speed can timely achieve grid dispatch and enhance stability of grid, which is a simple and economic way [5], [6]. So improving wind speed prediction accuracy is an effective measure to availably utilize wind energy and enhance safety and stability of grid.

The associate editor coordinating the review of this manuscript and approving it for publication was Dongbo Zhao.

Many scholars have focused on the research of wind speed prediction. Several prediction models have been developed in the past decades. In general, wind speed prediction models can be mainly classified into physical models, statistical models, artificial intelligence models and hybrid models [7].

Physical models mainly adopt the numerical weather prediction (NWP) data to forecast the wind speed of the considered site [8], [9]. They can obtain regional and global forecasts by using NWP data to solve the complex numerical systems. However, the NWP data cannot be easily obtained and have a long renewal period. They cannot meet the requirement of short term wind speed prediction and are often adopted for long term wind speed prediction.

Statistical models establish the functional model among time series data based on recursive theory [10]. They can easily capture the relationship according to historical data and are suitable for short term wind speed prediction. Autoregressive (AR) [11] and autoregressive moving

average (ARMA) [12] were widely applied for predicting wind speed, and narrower width of intervals and better performance were obtained compared with those of persistence model. But they are restricted in application for non-stationary time series. Autoregressive integrated moving average (ARIMA) [13] was developed for predicting non-stationary time series. The effectiveness of ARIMA was proven by predicting hour-ahead wind speed series in literature [14]. However, statistical models cannot always facilitate the competitive results for nonlinear patterns.

Artificial intelligence models developed rapidly recently for wind speed prediction due to their strong nonlinear fitting ability. The core parts in artificial intelligence models are artificial neural network (ANN), mainly including back propagation (BP) [15] and radial basic function (RBF) [16], recurrent neural network (RNN) [17] and so on. Several artificial intelligence models were applied for forecasting short term wind speed series in literature [18], and forecasting performances under different structures of networks were studied. ANN can capture the complex and key features hidden in wind speed series and derive nonlinear relationship among wind speed series. However, local minima and overfitting state are often caused [19] so that the prediction accuracy is limited. Least squares support vector machine (LSSVM) and Gaussian process were developed for forecasting wind speed series to overcome the above drawbacks in literature [20], [21]. And the results showed that LSSVM exhibited better performance than persistence model, Gaussian process was proven superior to RBF for estimating the upper and the lower bounds of wind speed. But the prediction accuracy of LSSVM and Gaussian process depend on the selection of the kernel function and parameters of kernel function in the model [22].

Owing to the complex characteristics of wind speed series and the limitation of single prediction model, many hybrid prediction models have been developed to enhance prediction accuracy of wind speed. The hybrid model based on ARIMA and ANN was established to forecast wind speed in literature [23], and the results show the superior prediction results were obtained compared with single ARIMA and ANN. With the development of intelligent search algorithm, such as genetic algorithm (GA) and practical swarm algorithm (PSO) and so on, the drawback of local optimization for many ANNs could be improved by combing intelligent search algorithm. The literature [24] combined GA and BP neural network to forecast 10-min and 1 h wind speed series, and the better forecasting performance was obtained compared with single BP neural network.

Almost wind speed prediction models mentioned above establish prediction model by directly using historical data. However, wind speed is influenced by atmospheric motion in reality, which brings certain disturbances and chaos characteristics to wind speed [25], [26], so atmospheric motion brings obstacles to accurate wind speed prediction. The literature [27] proposed that chaos characteristic is existed in short time wind speed time series, so the prediction accuracy of wind speed prediction model considering the chaos characteristics has been improved. For complex and nonlinear features of wind speed, many nonlinear analysis tools were developed. Decomposition-based methods, including wavelet transform (WT) [28], empirical mode decomposition (EMD) [29], and variational mode decomposition (VMD) [30] etc., were widely applied to pre-process wind speed data and obtain relatively stable subseries. The literature [31] adopted WT to preprocess wind speed series and build prediction model for separate components, but the effectiveness of WT depends on the empirical selection for wavelet basis function. EMD can adaptively decompose raw series into a series of relatively stable subseries, but the literature [32] pointed out that mode mixing occurs in decomposition process of EMD, so hybrid prediction model based on EMD is restricted. Ensemble empirical mode decomposition (EEMD) is a noise assisted data analysis method. Mode mixing existed in EMD can be effectively improved by using assisted Gaussian white noises. But the decomposition effect of EEMD is related to the amplitude and ensemble times of white noises. And there is no specific criterion for the selection to the amplitude and ensemble times of white noises at present [33]. VMD was applied to decompose raw wind speed series in literature [34], but the determination to the number of modes for VMD has no uniform criterion. The Lorenz equation and VMD are adopted in wind speed prediction model in literature [35], and the wind speed prediction accuracy has been improved. However, the Lorenz equation cannot describe the disturbance comprehensively and there isn't concrete criterion to the parameter selection of Lorenz equation to ensure the prediction accuracy. Thus, for predicting wind speed, the physical characteristics of actual wind speed need to be scientifically studied further. In addition, the prediction model based on decomposition method still have room to enhance.

Based on the above, a novel self-adaptive hybrid wind speed prediction model considering atmospheric motion and fractal feature is proposed in this paper. Firstly, physical characteristics of atmosphere motion on wind speed series is analyzed and described by Lorenz-Stenflo (LS) equation. By employing the optimization effect of one-dimension LS motion series, the effects of atmosphere motion are weakened during the process of EEMD decomposition to wind speed. Then the key parameter of LS equation is determined based on the Fractal Dimension (FD) of wind speed, which achieves the adaptivity to different wind speed series. The optimization mechanism considering atmosphere motion is analyzed from the distributions of extreme points and envelope curves of wind speed series. Finally, back propagation (BP) neural network is used for prediction. To conquer the drawback of falling into local optimum and over-fitting for BP neural network, BP neural network optimized by genetic algorithm (GA-BP) is adopted. Eight groups of wind speed data on different time scales (10-min interval, 30-min interval, 1-h interval and 2-h interval) from two wind farms of Abbotsford in Canada and Kansas in US are selected to test

and evaluate. The superiority and universality of proposed prediction model are verified compared with various prediction models.

The structure of this study is organized as follows: Section 2 introduces the theories of LS equation, EEMD, decomposition method considering atmospheric motion and GA-BP neural network. Section 3 introduces the key parameter in LS equation selection principle and mechanism analysis of decomposition method considering atmospheric motion. Section 4 compares and analyzes the prediction results of eight groups of wind speed data on different time scales among the proposed method and other benchmark models. Section 5 makes the conclusion and outlook.

II. RELATED METHODOLOGIES

A. DESCRIPTION OF ATMOSPHERIC MOTION-LS MOTION SERIES

In reality, atmospheric motion influences wind speed and brings certain disturbances and chaos characteristics to wind speed, so that wind speed series exhibits the features of uncertainty and volatility. Atmospheric system is the deterministic dynamic system, which can be described by deterministic equation. In this paper, for the disturbances and chaos effect caused by atmospheric motion on wind speed series, the LS equation is adopted to describe the characteristics of atmospheric motion. Lorenz equation is a simple differential equation to describe atmospheric fluid motion, it can capture the periodic and aperiodic chaos characteristics based on the deterministic equation [36]. The LS equation is developed from the Lorenz equation considering the rotation of airflow [37], which can be employed to describe the characteristics of atmospheric fluid motion more comprehensively. LS equation is shown as formula (1):

$$\begin{cases} \dot{x} = \alpha(y - x) + \gamma w \\ \dot{y} = x(r - z) - y \\ \dot{z} = xy - \beta z \\ \dot{w} = -x - \alpha w \end{cases} \tag{1}$$

where, x, y, z, w respectively represent the convection motion intensity, the temperature difference between upflow and downflow, the deviation of vertical gradient of average temperature, the rotation of airflow. α is the Prandtl number, r is the Rayleigh number, β is the geometrical parameter, γ is the rotation number. The LS equation remains unchanged under the transformation M: $(x, y, z, w) \rightarrow (-x, -y, -z, -w)$ and has symmetry about the z axis. In general, when LS is used to describe atmospheric system, α, β, γ have little effect on nonlinear system described by LS equation and are usually set to fixed values($\alpha = 10, \beta = 8/3, \gamma = 1$) [38], [39]. The value of r has a great effect. The atmospheric motion characteristics described by LS equation in different r are shown in table 1 [40].

As shown in table 1, the value of r has a great effect on atmospheric motion characteristics described by LS equation, so r is the key parameter. In addition, LS equation can represent the aperiodic and periodic chaos characteristics of the atmospheric system in different r, which is consistent with the characteristics that short term wind speeds have different chaos degrees on different time scales. That is different wind speed series show different fluctuation characteristics, which can be approximatively demonstrated by LS equation. And when the parameters of LS equation are set as some values, solve the LS equation, and the four-dimensional motion series x, y, z, w can be obtained, then normalize the four-dimensional motion series with formula (2):

TABLE 1. The atmospheric motion characteristics described by LS equation in different *r*.

Value of r	atmospheric fluid motion
$0< r <1$	Heat conduction
$1< r <13.97$	Convection motion
$13.97< r <24.74$	Transient chaos
$r >24.74$	Chaos

$$\begin{cases} \tilde{x} = \dfrac{x - x_{\min}}{x_{\max} - x_{\min}} \\ \tilde{y} = \dfrac{y - y_{\min}}{y_{\max} - y_{\min}} \\ \tilde{z} = \dfrac{z - z_{\min}}{z_{\max} - z_{\min}} \\ \tilde{w} = \dfrac{w - w_{\min}}{w_{\max} - w_{\min}} \end{cases} \tag{2}$$

where, x, y, z, w are the four-dimensional motion series, $x_{\max}, y_{\max}, z_{\max}, w_{\max}$ and $x_{\min}, y_{\min}, z_{\min}, w_{\min}$ are respectively maximums and minimums of x, y, z, w, $\tilde{x}, \tilde{y}, \tilde{z}, \tilde{w}$ are the normalized four-dimensional motion series. Assume that r is equal to 30 and the initial value of the system $[x_0, y_0, z_0, w_0]$ is equal to $[0.01, 0.01, 0.01, 0.01]$. The motion characteristics of the attractor is shown in figure 1.

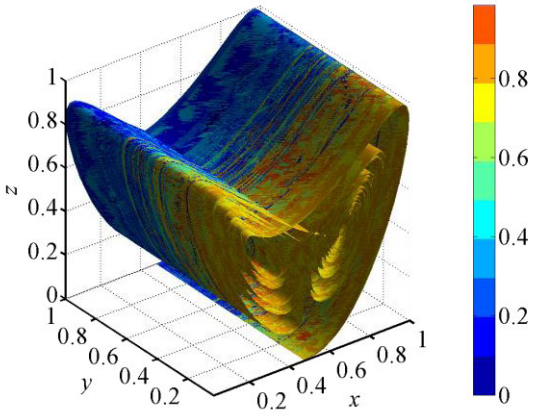

FIGURE 1. The motion characteristics of the attractor in $r = 30$.

As shown in figure 1, the motion of the attractor has large deviation compared with the initial value, which has

the uncertainty but varies within certain limits. The motion characteristics of the attractor in $r = 30$ exhibits the chaos characteristics. So the motion of the attractor in proper r can capture the chaos and transient chaos information of short term wind speed series. Because wind speed series is one-dimensional time series, so we map four-dimensional motion series into one-dimensional motion series by using Manhattan Distance method in formula (3) so that the one-dimensional motion series contain the information of $\tilde{x}, \tilde{y}, \tilde{z}, \tilde{w}$, and better describe the effect of atmospheric motion on wind speed. Figure 2 shows the one-dimensional LS motion series d_{LS} in $r = 22$ and $r = 45$. As shown in figure 2, the trend of the one-dimensional LS equation motion series all have a large deviation from the initial value, which reflects certain disturbances and chaos characteristics. According to Table 1, it reflects the transient chaos characteristics in $r = 22$ for the one-dimensional LS motion series d_{LS}. And the chaos characteristics is reflected in $r = 45$ for d_{LS}. So the disturbances and chaos effect of atmospheric motion on wind speed can be described by the characteristics of the one-dimensional LS motion series d_{LS}.

$$d_{\mathrm{LS}} = |\tilde{x} - \tilde{x}_0| + |\tilde{y} - \tilde{y}_0| + |\tilde{z} - \tilde{z}_0| + |\tilde{w} - \tilde{w}_0| \qquad (3)$$

where, $\tilde{x}_0, \tilde{y}_0, \tilde{z}_0, \tilde{w}_0$ are normalized initial value of the system, d_{LS} is one-dimensional LS equation motion series.

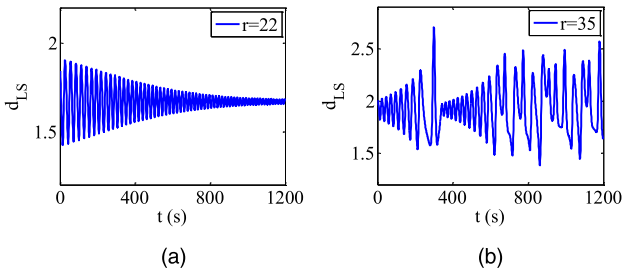

FIGURE 2. The one-dimensional LS motion series d_{LS}.(a) $r = 22$; (b) $r = 45$.

B. EEMD

EMD [41] is an adaptive signal decomposition method for nonlinear and nonstationary time series by Huang *et al.* It can decompose the time series into a number of intrinsic mode functions (IMFs) and a residue. The IMFs and residue reflect different time scales in the original time series. However, mode mixing may easily occur for EMD, which will cause EMD to be limited in applications.

EEMD [42] is a noise assisted data analysis method. By using assisted white noises, EEMD can smooth pulse disturbances, noises and other abnormal events, maintain the distribution of extreme points of the time series more uniform, which can improve mode mixing problem of EMD. Because the white noises added to time series have characteristics of zero mean, the result of ensemble mean is the decomposition result of the time series. The details can be seen in [42].

C. DECOMPOSITION OF WIND SPEED BY EEMD OPTIMIZED WITH LS EQUATION

Although EEMD has improved the mode mixing effect of EMD to some extent, the IMFs of wind speed time series obtained by directly using EEMD still cannot reflect the true time scales due to the effect of atmospheric motion. The high-frequency IMFs obtained by EEMD have certain chaos and poor regularity so that the prediction accuracy of wind speed based on EEMD can't be improved effectively. To solve the problem, the one-dimension LS motion series d_{LS} is adopted to describe chaos information in wind speed and improves the decomposition process of wind speed by EEMD, which is called LS-EEMD. The concrete process of LS-EEMD is: set the initial value and parameters of LS equation, solve the LS equation and obtain one-dimension LS motion series d_{LS}; then subtract the one-dimensional LS motion d_{LS} series from the wind speed series, decompose the new series by EEMD and then add the one-dimensional LS motion series to the residue of the EEMD so that the decomposition result is still the decomposition result of the original wind speed series. Because the disturbances and chaos effect existed in wind speed can be weakened before decomposition by LS-EEMD, the IMFs that better reflect the true time scales in wind speed series can be obtained.

D. D GA-BP NEUTRAL NETWROK

Back propagation (BP) neutral network is one of the most commonly used artificial neural network models, which consists of input layer, hidden layers and output layer. It concludes two parts: forward propagation and error back propagation. The inputs are passed layer by layer by forward propagation. The outputs go back to the input layer by error back propagation if a large error occurs between the output value and expected value. The details can be seen in literature [29]. BP neural network may easily enter the state of falling into local optimum and over-fitting in predicting wind speed series. Genetic algorithm (GA) can be adopted to improve the drawback of BP neural network due to its global optimization ability. The initial weights and threshold values of BP neutral network can be optimized by GA. The GA-BP model is shown in figure 3.

III. SELECTION TO THE KEY PARAMETER IN LS-EEMD AND MECHANISM ANALYSIS FOR FD-LS-EEMD

A. FD-LS-EEMD

When LS-EEMD is used to improve the decomposition process of wind speed by EEMD, α, β, γ have little effect on the decomposition effect of LS-EEMD and are set to fixed values. The value of r has a great effect on decomposition effect of LS-EEMD. Different wind speed series contain different degrees of atmospheric disturbances and chaos. So LS-EEMD needs to adaptively select the value of r according to effect degrees of atmospheric disturbances and chaos on wind speed series. So r is the key parameter.

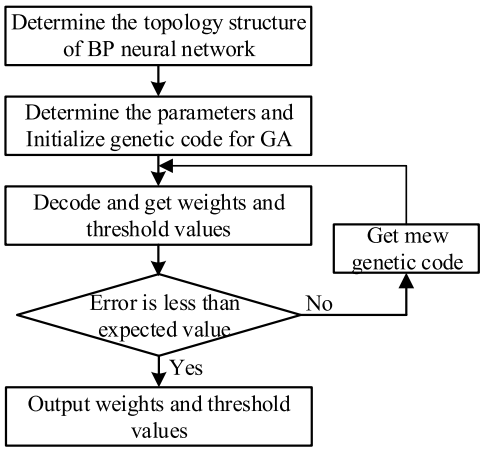

FIGURE 3. The structure of GA-BP neural network model.

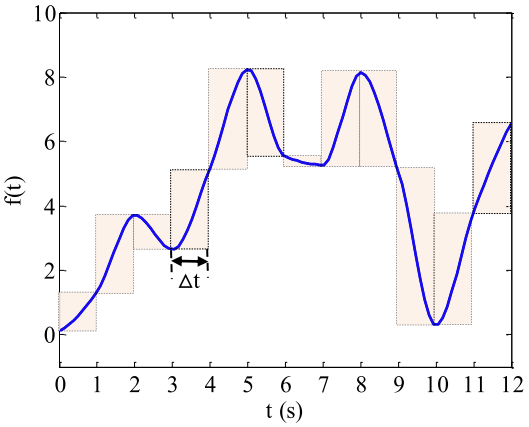

FIGURE 4. Arbitrary signal covered by rectangles with a specific time interval in calculating fractal dimension.

Fractal dimension is a mathematical method to reveal the distribution characteristics and complexity of elements in different scales [43]. Fractal dimension is related to chaos and can have a quantitative analysis to the randomness and irregularity of the signal. The fractal dimension is sensitive to variation of time series. Meanwhile, the calculation of fractal dimension needs less parameters and does not need the process of the phase space reconstruction. So we try to adopt the fractal feature of wind speed series to select the key parameter in LS-EEMD, and the optimized LS-EEMD by calculation fractal dimension is called FD-LS-EEMD.

Box-counting dimension algorithm is a classical method to calculate fractal dimension [44]. The Hurst index H is an important parameter in box-counting dimension method. The relationship between fractal dimension D and H is:

$$D = 2 - H \tag{4}$$

where, D is the fractal dimension; H is the Hurst index.

H can be calculated according to the equation (5):

$$H = \lim_{\Delta t \to 0} \frac{\lg N(\Delta t)}{\Delta t} = \lim_{\Delta t \to 0} \frac{N(\Delta t)/\Delta t^2}{\lg(1/\Delta t)} \tag{5}$$

$$N(\Delta t) = \sum_{i=0}^{n-1} |f(t_i + \Delta t) - f(t_i)| \Delta t \tag{6}$$

where, $f(t_i)$ is the value of time series at t_i; $N(\Delta t)$ is the rectangle area; n is the data number in Δt.

So D can be denoted as formula (7):

$$D = \lim_{\Delta t \to 0} (2 - \frac{\lg N(\Delta t)}{\Delta t}) = \lim_{\Delta t \to 0} \frac{\lg(N(\Delta t)/\Delta t^2)}{\lg(1/\Delta t)} \tag{7}$$

Figure 4 shows the process of calculating its fractal dimension for an arbitrary signal. After selecting a specific time interval Δt, $|f(t_i + \Delta t) - f(t_i)|$ reflects the fluctuation degree of the time series, $N(\Delta t)$ reflects the rectangle's coverage degree of the time series in time interval Δt.

To verify the quantitative analysis role to the randomness and irregularity of the series by the fractal dimension, 10-min interval wind speed series from 301 to 450 in Abbotsford wind farm is adopted for analysis as it contains different degrees of volatility and complexity of wind speed series. Figure 5 shows the distribution of 10-min interval wind series from 301 to 450.

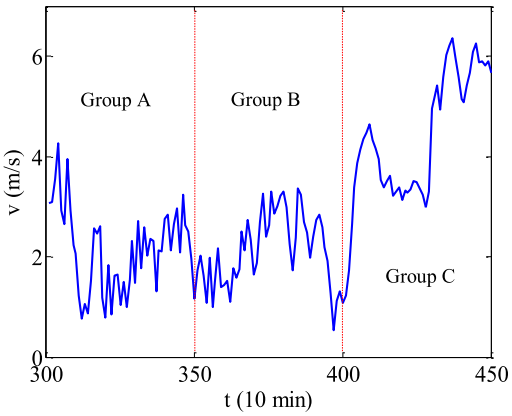

FIGURE 5. The distribution of 10-min interval wind series from 301 to 450 in Abbotsford wind farm.

The 150 points in figure 5 are divided into three groups for easy analysis: Group A from 301 to 350; Group B from 351 to 400; Group C from 401 to 450. There are only 50 points for every group so that the degree of volatility and complexity of every group can be intuitively observed. As can be seen, Group A and Group B are relatively close in data complexity. They have stronger volatility compared with Group C. And data of Group A have slightly stronger variation compared with those of Group B. The data of Group C has stronger correlation and weaker complexity. Despite of larger amplitudes, the data of Group C changes more slowly and has better correlation among data. As the time interval Δt should be set as small as possible in calculating fractal dimension, the time interval Δt is set as 1 here. The fractal dimensions of three groups of data are calculated by using the box-counting dimension algorithm, and the results are shown in table 2.

As shown in table 2, the fractal dimensions of Group A and Group B are close and the fractal dimension of Group C is the

TABLE 2. Fractal dimensions of three groups of data.

Wind speed	D
Group A	1.3926
Group B	1.3831
Group C	1.1861

smallest. This indicates that the smaller the fractal dimension is, the stronger the correlation among data points is. The random fluctuation of group A and group B is stronger, and the correlation among data is weaker so that they have larger fractal dimensions. By comparing the data of Group A and Group B, the data of Group A vary slightly quickly at about 322-333 so that the fractal dimension of the data of Group A is slightly larger than that of the data of Group B. Therefore, the fractal dimension can be used to quantificationally describe the degree of volatility and complexity of wind speed series. The wind speed series with stronger volatility have weaker correlation among data so that they have larger fractal dimension. The wind speed series with weaker volatility tend to have stronger correlation among data points so that they have smaller fractal dimension.

According to the correlation of fractal dimension and the volatility and complexity of wind speed series, the fractal feature of wind speed can be developed to determine the key parameter of LS equation. Thus, FD-LS-EEMD solves the problem of selection to the fixed key parameter r of LS-EEMD and is more adaptive than LS-EEMD. And FD-LS-EEMD realizes the effectiveness to different wind speed series based on the fractal feature. The main process for FD-LS-EEMD is: set the initial value and α, β, γ of LS equation, set r as a small value (As known in Table 1, r needs to exceed 13.97). When the wind speed series that subtracted the one-dimension LS motion series has been decomposed by EEMD, calculate the fractal dimensions of IMFs. The decomposition process for FD-LS-EEMD is finished if the fractal dimensions of IMFs obtained by FD-LS-EEMD are less than that by EEMD. Or else increase the value of r until the condition is met. Because the prediction errors by EEMD are mainly existed in high-frequency IMFs, the first three IMFs are required to meet the condition to reduce calculation time. The wind speed decomposition by FD-LS-EEMD is shown in figure 6.

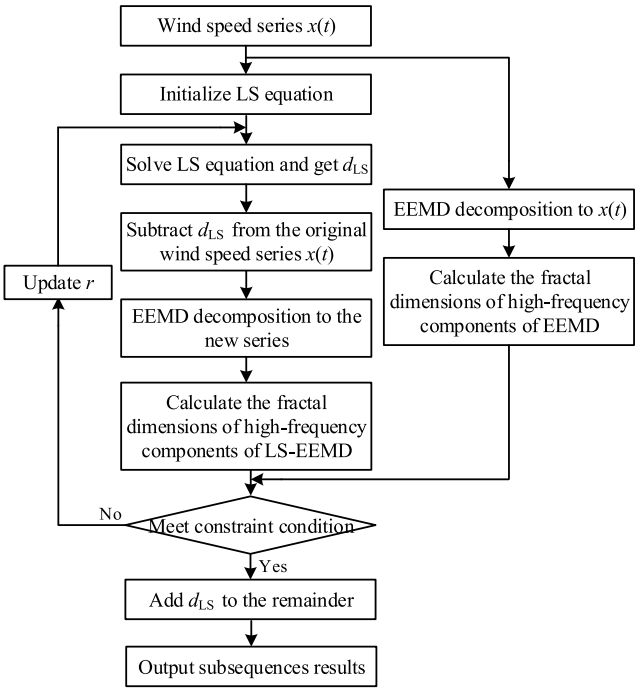

FIGURE 6. The wind speed decomposition by FD-LS-EEMD.

B. MECHANISM ANALYSIS FOR FD-LS-EEMD

EMD decomposes wind speed series by finding the extreme points of the series and sieving mean envelope curves. For actual wind speed series, the abnormal extreme points are existed in wind speed series due to the atmospheric disturbances and noises. The overshoot and undershoot of envelope curves will occur so that the IMFs cannot maintain the true time scales, which caused the mode mixing problem [45]. EEMD can improve the distribution of the extreme points of the wind speed series by using assisted white noises, but there is still no specific basis about the selection to the amplitude and ensemble times of white noises. The abnormal extreme points are still existed. The decomposition effects are unsatisfactory so the prediction accuracy is limited. The disturbances and chaos effects caused by atmospheric motion on wind speed are considered for FD-LS-EEMD, it can weaken atmospheric motion effects on the wind speed series. Based on the fractal feature of wind speed, FD-LS-EEMD can maintain the distribution of extreme points more uniform and improve the problem of overshoot and undershoot of envelope curves of EMD and EEMD for different wind speed series. So FD-LS-EEMD can obtain IMFs that better maintain the true time scales of wind speed series. To illustrate the superiority of FD-LS-EEMD compared with EMD and EEMD, the upper envelope curves respectively obtained with EMD, EEMD and FD-LS-EEMD for 10-min interval wind speed series in Abbotsford wind farm are shown in figure 7.

As shown in figure 5, the distribution of extreme points is very nonuniform and the problem of overshoot of envelope curve occurs at about 534-538 and 548-555 for EMD, and the abnormal extreme point occurs at 540. So the envelope curve isn't very smooth and has the problem of overshoot of envelope curve with EMD. The problem of overshoot of envelope curve occurred at about 534-538 and 548-555 is improved by EEMD. And the abnormal extreme point occurs at 540 is eliminated. However, white noises may cause abnormal extreme points, such as the 559th point. So EEMD can improve the distribution of extreme points with assisted white noises, but the envelope curve still isn't enough smooth. Due to weakening disturbances and noises caused by atmospheric motion, the problem of overshoot of envelope

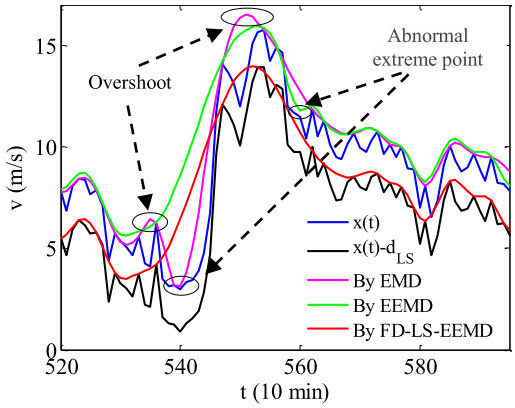

FIGURE 7. Distribution of upper envelope curves obtained with three decomposition methods for 10-min interval wind speed.

curve occurred at about 534-538 and 548-555 is obviously improved, the problem of unsmooth envelope curve caused by abnormal extreme point at the 559th point is solved meanwhile. So FD-LS-EEMD can obtain IMFs that better maintain true time scales.

IV. CASE STUDY

A. DATA SETS

As the accuracy of wind speed prediction is influenced by different wind farms. Eight groups of wind speed data on different time scales from Abbotsford wind farm and Kansas wind farm are selected for analysis in this paper. There are 1200 wind data for every group. The first 1100 wind speed data are used to train model and the last 100 wind speed data are tested and evaluated.

B. PREDICTION MODEL AND EVALUATION INDICES

Considering the disturbances and chaos effects caused by atmospheric motion on wind speed, FD-LS-EEMD is employed to pre-process wind series, then GA-BP neural network is adopted to predict every IMF and residue. So a wind speed prediction model based on FD-LS-EEMD and GA-BP neural network is developed.

To effectively evaluate the effectiveness of the proposed prediction model, Mean Absolute Percentage Error (MAPE), Mean Absolute Error (MAE) and Root Mean Square Error (RMSE) are used for analysis. Smaller values of MAPE, MAE and RMSE correspond to better prediction performance of the model. The evaluation indices are shown as follows:

$$MAPE = \frac{\sum_{i=1}^{n} \frac{|p(i)-c(i)|}{c(i)}}{n} * 100\% \tag{8}$$

$$MAE = \frac{\sum_{i=1}^{n} |c(i) - p(i)|}{n} \tag{9}$$

$$RMSE = \sqrt{\frac{\sum_{i=1}^{n} (p(i) - c(i))^2}{n}} \tag{10}$$

where, $p(i)$ is the prediction value, $c(i)$ is the actual value, n is the number of data.

In addition, to exhibit the effectiveness of various prediction models, the improvement relative to the persistent model is analyzed between the persistent model and other models from MAPE, MAE and RMSE. The improvement indices can directly reveal the superiority degree of various prediction models. The improvement is:

$$Improvement = \frac{EI_{persistent} - EI}{EI_{persistent}} \times 100\% \tag{11}$$

where $EI_{persistent}$ and EI respectively stand for values of error indices got by persistent model, and values of error indices got by other models considered in this paper.

C. NUMERICAL RESULTS AND ANALYSIS

To verify the superiority of the proposed prediction model, GA-BP neural network, EEMD-GA-BP neural network and LS-EEMD-GA-BP neural network are firstly established for comparison. Due to strong randomness and volatility for most wind speed series, chaos characteristics are mainly existed in wind speed series, so r is set as 25 for LS-EEMD-GA-BP neural network here.

Figure 8 and figure 9 respectively show the prediction results of wind speed for the two wind farms. As shown in figure 8 and figure 9, all of the original wind speed series represented with blue curve have the characteristics of volatility and non-stationary, which reflect the actual wind speed is affected by atmospheric motion. The prediction results generated by GA-BP neural network lag behind the actual values for some wind data, so the prediction values and actual values have the large deviations. The three decomposition-based prediction models have obviously improved prediction effect of GA-BP neural network. Compared with EEMD-GA-BP neural network and LS-EEMD-GA-BP neural network, the proposed prediction model gets the least deviations between prediction values and actual values. This is because FD-LS-EEMD can adaptively select the one-dimension LS motion series d_{LS}, which can effectively improve the decomposition process of wind speed by EEMD, weaken the disturbances and chaos effect caused by atmospheric motion on wind speed and enhance the smooth degree of IMFs. So the prediction results are more reliable by the proposed model compared with other models.

Aside from prediction effect figures, error indices could have a quantitative analysis to prediction model. Persistent model, LSTM and DWT-GA-BP neural network are also introduced for comparison. Table 3 shows error indices and run time (T) generated by seven prediction models for two wind farms. The prediction errors generated by GA-BP neural network and LSTM are obviously less compared with those by persistent model. Although GA-BP neural network has larger prediction errors generally, it needs less run time so that it is more suitable for hybrid models. For decomposition-based prediction models, EEMD-GA-BP neural network has better prediction effects compared with those obtained

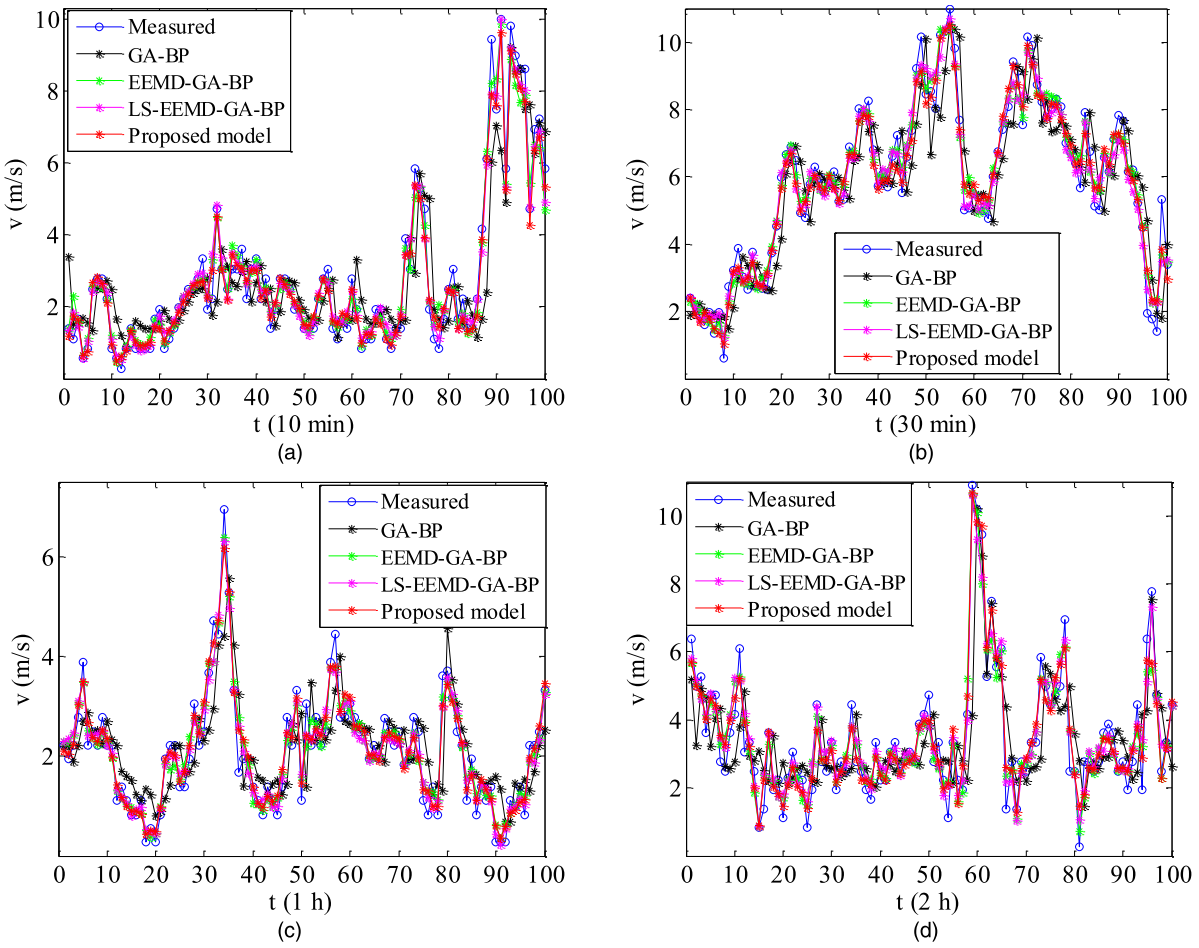

FIGURE 8. The wind prediction result for Kansas wind farm; (a) 10-min interval; (b) 30-min interval; (c) 1-h interval; (d) 2-h interval.

by DWT-GA-BP neural network in general. Due to the fixed r for LS-EEMD, LS-EEMD-GA-BP neural network has different prediction effects on different wind series. For example, the MAPEs of EEMD-GA-BP neural network and LS-EEMD-GA-BP neural network for 10-min interval wind in Abbotsford farm are respectively 13.02% and 10.36%. However, the MAPEs of EEMD-GA-BP neural network and LS-EEMD-GA-BP neural network for 1-h interval wind in Kansas farm are respectively 11.09% and 11.81%, which verifies the importance of the key parameter r in LS equation. And the best prediction effects are generated by the proposed model for two wind farms.

For the run time, owing to the prediction to every subsequence for decomposition-based models, several decomposition-based prediction models need more time compared with that of GA-BP neural network. They have close run time for EEMD-GA-BP neural network and LS-EEMD-GA-BP neural network, this is because the optimization to EEMD by the fixed one-dimension LS motion series d_{LS} needs little time. The proposed model needs slightly more time compared with other two hybrid models due to the search for the key parameter r, but the cost can be tolerated considering the obvious enhancement of the prediction accuracy since the calculation time can still meet the requirement of short term wind speed prediction in practice.

Meanwhile, table 4 shows the improvements of other prediction models with respect to the persistent model. As shown in table 4, all of the prediction models achieve different improvement levels relative to the persistent model for eight groups of wind speed series in two wind farms. Taking 10-min wind speed series in Abbotsford wind farm for example, the MAPE improvements of LSTM, GA-BP neural network, DWT-GA-BP neural network, EEMD-GA-BP neural network, LS-EEMD-GA-BP neural network and proposed model relative to the persistent model respectively are 42.24%,39.66%, 63.36%, 66.43%, 73.29% and 75.27%. The MAE improvements respectively are 25.30%, 22.21%, 63.41%, 65.39%, 67.70% and 69.59%. Through the improvements of different prediction models relative to persistent model for the eight cases, the proposed prediction model exhibits the greatest improvement compared to other models. It is demonstrated that the proposed prediction model has better ability of capturing the complex

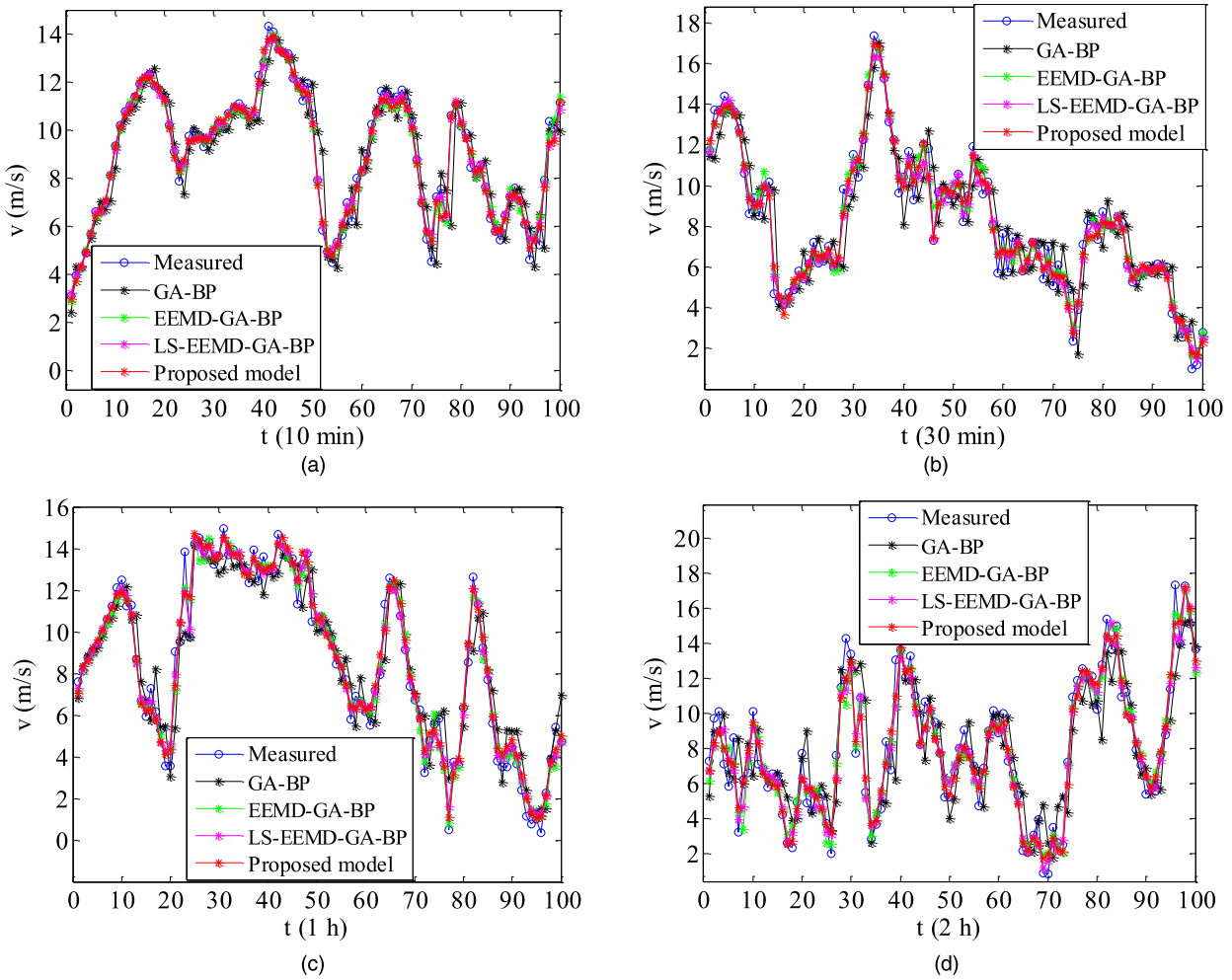

FIGURE 9. The wind prediction result for Kansas wind farm; (a) 10-min interval; (b) 30-min interval; (c) 1-h interval; (d) 2-h interval.

features and better prediction effectiveness for wind speed series.

To further reveal the reason of the perfect performance for the proposed prediction model, the selected one-dimension motion series and characteristics of obtained high frequency IMFs by proposed FD-LS-EEMD are analyzed. Taking wind speed series in Abbotsford wind farm for example, figure 10 shows the selected one-dimension motion series d_{LS} for four groups of wind series in Abbotsford wind farm by FD-LS-EEMD. As shown in figure 10, FD-LS-EEMD selects the different one-dimension motion series d_{LS} that is suitable for every group of wind speed series. It is demonstrated that different wind series contain different degrees of atmospheric disturbances and chaos for actual wind speed, so that they exhibit different degrees of volatility and non-stationary. Based on the role of quantitative analysis of fractal feature to the randomness and irregularity of the wind series, FD-LS-EEMD can adaptively select proper one-dimension motion series d_{LS} and achieve the effectiveness for different wind speed series. So FD-LS-EEMD is self-adaptive to wind speed. Then figure 11 shows the fractal dimensions of high-frequency IMFs obtained by EEMD and

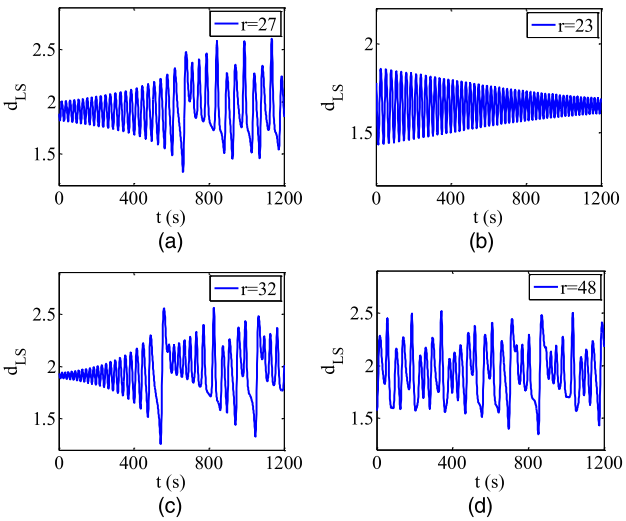

FIGURE 10. The injected one-dimension d_{LS} motion series for wind series in Abbotsford wind farm by FD-LS-EEMD; (a)10-min interval; (b)30-min interval; (c)1-h interval; (d)2-h interval.

FD-LS-EEMD for four groups of wind series in Abbotsford wind farm. As shown in figure 11, for every decomposition

TABLE 3. Prediction errors generated by several models for two wind farms.

Wind speed	Model	Abbotsford wind farm				Kansas wind farm			
		MAPE (%)	MAE (m/s)	RMSE (m/s)	T (s)	MAPE (%)	MAE (m/s)	RMSE (m/s)	T (s)
10-min interval	Persistent	38.78	0.8740	1.1603	<1	10.31	0.8042	1.0644	<1
	LSTM	22.40	0.6529	0.8591	62	7.09	0.6523	0.8988	59
	GA-BP	23.40	0.6799	0.8680	17	7.26	0.6744	0.9282	16
	DWT-GA-BP	14.21	0.3198	0.4100	118	3.89	0.2748	0.4140	110
	EEMD-GA-BP	13.02	0.3025	0.3982	136	2.84	0.2388	0.3284	120
	LS-EEMD-GA-BP	10.36	0.2823	0.3622	136	2.89	0.2253	0.3065	121
	Proposed model	9.59	0.2658	0.3530	142	2.40	0.2157	0.2918	132
30-min interval	Persistent	18.72	0.8446	1.1053	<1	18.46	1.1693	1.1358	<1
	LSTM	13.36	0.5715	0.7027	60	17.53	1.0966	1.0188	60
	GA-BP	14.81	0.6623	0.8830	16	18.10	1.0943	1.0115	16
	DWT-GA-BP	8.17	0.3515	0.4027	113	7.11	0.4217	0.5359	111
	EEMD-GA-BP	9.63	0.3600	0.4222	134	7.71	0.4562	0.5595	131
	LS-EEMD-GA-BP	9.82	0.3650	0.4323	136	7.22	0.4481	0.5626	132
	Proposed model	7.67	0.3258	0.3629	138	6.58	0.4163	0.5145	140
1-h interval	Persistent	39.69	0.6351	0.8551	<1	29.12	1.3193	1.9324	<1
	LSTM	29.23	0.5343	0.6816	62	24.12	1.0071	1.4632	61
	GA-BP	30.21	0.5478	0.6999	16	23.74	0.9876	1.4568	17
	DWT-GA-BP	18.54	0.2808	0.3515	117	11.84	0.5413	0.7311	116
	EEMD-GA-BP	16.83	0.2450	0.3072	130	11.09	0.4484	0.5714	130
	LS-EEMD-GA-BP	16.27	0.2307	0.2894	130	11.81	0.4535	0.5746	130
	Proposed model	16.02	0.2258	0.2800	140	8.52	0.3760	0.4968	145
2-h interval	Persistent	39.59	0.9317	1.1792	<1	31.73	1.9295	2.4061	<1
	LSTM	31.29	0.8076	0.9693	61	25.04	1.4199	1.8320	61
	GA-BP	33.50	0.8569	1.0135	17	30.08	1.5590	2.0995	17
	DWT-GA-BP	18.76	0.4452	0.4752	117	17.06	0.9196	1.1576	117
	EEMD-GA-BP	17.40	0.4116	0.4275	125	14.18	0.7761	0.9785	134
	LS-EEMD-GA-BP	17.44	0.4105	0.4302	127	13.94	0.7420	0.9698	134
	Proposed model	16.45	0.4032	0.3975	142	11.81	0.6949	0.9084	150

TABLE 4. Improvement relative to the persistent model for other prediction models.

Wind speed	Model	Abbotsford wind farm			Kansas wind farm		
		MAPE	MAE	RMSE	MAPE	MAE	RMSE
10-min interval	LSTM	42.24	25.30	25.96	31.23	18.89	15.56
	GA-BP	39.66	22.21	25.19	29.58	16.14	12.80
	DWT-GA-BP	63.36	63.41	64.66	62.27	65.83	61.10
	EEMD-GA-BP	66.43	65.39	65.68	72.45	70.31	69.15
	LS-EEMD-GA-BP	73.29	67.70	68.78	71.97	71.98	71.20
	Proposed model	75.27	69.59	69.58	76.72	73.18	72.59
30-min interval	LSTM	28.63	32.33	36.42	5.04	6.22	10.30
	GA-BP	20.89	21.58	20.11	1.95	6.41	10.94
	DWT-GA-BP	56.36	58.38	63.57	61.48	63.94	52.82
	EEMD-GA-BP	48.56	57.38	61.80	58.23	60.99	50.74
	LS-EEMD-GA-BP	47.54	56.78	60.89	60.89	61.68	50.47
	Proposed model	59.03	61.43	67.17	64.36	64.40	54.70
1-h interval	LSTM	26.35	15.87	20.29	17.17	23.66	24.28
	GA-BP	23.89	13.75	18.15	18.48	25.14	24.61
	DWT-GA-BP	53.29	55.79	58.89	59.34	58.97	62.17
	EEMD-GA-BP	57.60	61.42	64.07	61.92	66.01	70.43
	LS-EEMD-GA-BP	59.01	63.68	66.16	59.44	65.63	70.26
	Proposed model	59.64	64.45	67.26	70.74	71.50	74.29
2-h interval	LSTM	20.96	13.32	17.80	21.08	26.41	23.86
	GA-BP	15.38	8.03	14.05	5.20	19.20	12.74
	DWT-GA-BP	52.61	52.22	59.70	46.23	52.34	51.89
	EEMD-GA-BP	56.05	55.82	63.75	55.31	59.78	59.33
	LS-EEMD-GA-BP	55.95	55.94	63.52	56.07	61.54	59.69
	Proposed model	58.45	56.72	66.29	62.78	63.99	62.25

method, the fractal dimensions of IMFs gradually decrease with the declining of frequency for the four groups of wind speed series. This is because the volatility degree of IMFs gradually reduces and the smooth degree of IMFs gradually

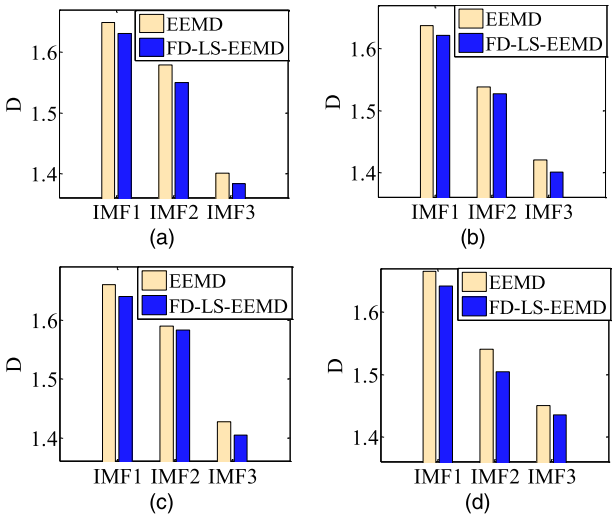

FIGURE 11. The fractal dimensions of high-frequency IMFs obtained by FD-LS-EEMD and EEMD for the four groups of wind series in Abbotsford wind farm. (a)10-min interval ($r = 27$); (b)30-min interval ($r = 23$); (c)1-h interval ($r = 32$); (d)2-h interval ($r = 48$).

enhances with the declining of IMFs' frequencies, which confirms the quantitative analysis role to the randomness and irregularity of the series by fractal dimension. Furthermore, the fractal dimensions of all high-frequency IMFs obtained by FD-LS-EEMD are less than those obtained by EEMD for the four groups of wind speed series, which indicates the superiority of FD-LS-EEMD compared with EEMD. Therefore, FD-LS-EEMD can effectively weaken disturbances and chaos effect of atmospheric motion from the raw wind series and facilitate the more regular subsequences. So the proposed prediction model can exhibit the promising prediction effect.

V. CONCLUSION AND OUTLOOK

The atmospheric motion system is a complex and nonlinear system, which brings disturbances and chaos effect to actual wind speed. To enhance accuracy of wind speed prediction, it is very valuable to predict wind speed considering its physical characteristics. Therefore, the wind speed prediction model based on FD-LS-EEMD and GA-BP neural network was proposed in this paper. LS equation was employed to describe the disturbances and chaos effect caused by atmospheric motion on wind speed, which could capture chaos and transient chaos information from wind speed series. Owing to improved distribution of extreme points of wind speed series by using one-dimension LS motion series, FD-LS-EEMD effectively weakened the effect of atmospheric motion on wind speed. The criterion based on fractal feature ensured the accurate selection of the key parameter in atmospheric motion equation according to different features of sampled wind data. Finally, the proposed prediction model achieved promising prediction accuracy by evaluating eight groups of wind speed series in two wind farms.

However, there are still some issues to be discussed further. So we will focus on the following aspects in the future work. (1) The initial value of LS equation is set to fixed value in this paper, and the influence of initial value of LS equation in the practical application needs to be discussed. (2) The four groups of wind speed series on different time scales are tested, and wind speed series on more time scales need to be researched to decide whether the proposed model is suitable to wind speed series on any time scale. (3) The optimization to the calculation time of the proposed model needs the further research.

REFERENCES

[1] P. Vithayasrichareon, J. Riesz, and I. MacGill, "Operational flexibility of future generation portfolios with high renewables," *Appl. Energy*, vol. 206, pp. 32–41, Nov. 2017.
[2] R. Li and Y. Jin, "A wind speed interval prediction system based on multi-objective optimization for machine learning method," *Appl. Energy*, vol. 228, pp. 2207–2220, Oct. 2018.
[3] Global Wind Energy Council (GWEC)[DB/OL], Brussels, Belgium. (2017). [Online]. Available: http//gwec.net/
[4] M. Lei, L. Shiyan, J. Chuanwen, L. Hongling, and Z. Yan, "A review on the forecasting of wind speed and generated power," *Renew. Sustain. Energy Rev.*, vol. 13, no. 4, pp. 915–920, May 2009.
[5] P. Kou, F. Gao, and X. Guan, "Sparse online warped Gaussian process for wind power probabilistic forecasting," *Appl. Energy*, vol. 108, pp. 410–428, Aug. 2013.
[6] Z. D. Tian, S. J. Li, Y. H. Wang, and X. W. Gao, "Short-term wind speed combined prediction for wind farms based on wavelet transform," *Trans. China Electrotechn. Soc.*, vol. 30, no. 9, pp. 112–120, 2015.
[7] F. M. Noman, G. A. Alkawsi, D. Abbas, A. A. Alkahtani, S. K. Tiong, and J. Ekanayake, "Comprehensive review of wind energy in malaysia: Past, present, and future research trends," *IEEE Access*, vol. 8, pp. 124526–124543, 2020.
[8] Y.-K. Wu, P.-E. Su, T.-Y. Wu, J.-S. Hong, and M. Yusri Hassan, "Probabilistic wind-power forecasting using weather ensemble models," *IEEE Trans. Ind. Appl.*, vol. 54, no. 6, pp. 5609–5620, Dec. 2018.
[9] H. Wang, S. Han, Y. Liu, J. Yan, and L. Li, "Sequence transfer correction algorithm for numerical weather prediction wind speed and its application in a wind power forecasting system," *Appl. Energy*, vol. 237, pp. 1–10, Mar. 2019.
[10] Z. H. Tang, G. N. Zhao, G. Wang, and T. H. Ouyang, "Hybrid ensemble framework for short-term wind speed forecasting," *IEEE Access*, vol. 8, pp. 45271–45290, 2020.
[11] O. Ait Maatallah, A. Achuthan, K. Janoyan, and P. Marzocca, "Recursive wind speed forecasting based on hammerstein auto-regressive model," *Appl. Energy*, vol. 145, pp. 191–197, May 2015.
[12] E. Erdem and J. Shi, "ARMA based approaches for forecasting the tuple of wind speed and direction," *Appl. Energy*, vol. 88, no. 4, pp. 1405–1414, Apr. 2011.
[13] K. Yunus, T. Thiringer, and P. Chen, "ARIMA-based frequency-decomposed modeling of wind speed time series," *IEEE Trans. Power Syst.*, vol. 31, no. 4, pp. 2546–2556, Jul. 2016.
[14] A. Sfetsos, "A novel approach for the forecasting of mean hourly wind speed time series," *Renew. Energy*, vol. 27, no. 2, pp. 163–174, Oct. 2002.
[15] Z.-H. Guo, J. Wu, H.-Y. Lu, and J.-Z. Wang, "A case study on a hybrid wind speed forecasting method using BP neural network," *Knowl.-Based Syst.*, vol. 24, no. 7, pp. 1048–1056, Oct. 2011.
[16] P. Jiang, Y. Wang, and J. Wang, "Short-term wind speed forecasting using a hybrid model," *Energy*, vol. 119, pp. 561–577, Jan. 2017.
[17] T. G. Barbounis and J. B. Theocharis, "Locally recurrent neural networks for long-term wind speed and power prediction," *Neurocomputing*, vol. 69, nos. 4–6, pp. 466–496, Jan. 2006.
[18] G. Li and J. Shi, "On comparing three artificial neural networks for wind speed forecasting," *Appl. Energy*, vol. 87, no. 7, pp. 2313–2320, Jul. 2010.
[19] M.-R. Chen, G.-Q. Zeng, K.-D. Lu, and J. Weng, "A two-layer nonlinear combination method for short-term wind speed prediction based on ELM, ENN, and LSTM," *IEEE Internet Things J.*, vol. 6, no. 4, pp. 6997–7010, Aug. 2019.
[20] J. Y. Zhou, J. Shi, and G. Li, "Fine tuning support vector machines for short-term wind speed forecasting," *Energy Convers Manag*, vol. 52, pp. 352–361, 2004.
[21] J. Yan, K. Li, E. W. Bai, J. Deng, and A. M. Foley, "Hybrid probabilistic wind power forecasting using temporally local Gaussian process," *IEEE Trans. Sustain. Energy*, vol. 7, no. 1, pp. 87–95, Dec. 2016.

[22] Z. C. Shi, H. Liang, and V. Dinavahi, "Wavelet neural network based multi objective interval prediction for short-term wind speed," *IEEE Access*, vol. 6, pp. 63352–63365, 2018.
[23] E. Cadenas and W. Rivera, "Wind speed forecasting in three different regions of mexico, using a hybrid ARIMA–ANN model," *Renew. Energy*, vol. 35, no. 12, pp. 2732–2738, Dec. 2010.
[24] S. Wang, N. Zhang, L. Wu, and Y. Wang, "Wind speed forecasting based on the hybrid ensemble empirical mode decomposition and GA-BP neural network method," *Renew. Energy*, vol. 94, pp. 629–636, Aug. 2016.
[25] L. Tan, J. Han, and H. Zhang, "Ultra-Short-Term wind power prediction by salp swarm algorithm-based optimizing extreme learning machine," *IEEE Access*, vol. 8, pp. 44470–44484, 2020.
[26] Z. D. Tian, S. J. Li, Y. H. Li, and X. W. Gao, "Chaos characteristics analysis and prediction for short-term wind speed time series," *Acta Phys. Sin*, vol. 64, no. 3, pp. 236–247, 2015.
[27] X. Q. Zhang and J. Liang, "Chaotic characteristics analysis and prediction model study on wind power time series," *Acta Phys. Sin*, vol. 61, no. 19, pp. 70–81, 2012.
[28] D. Liu, D. Niu, H. Wang, and L. Fan, "Short-term wind speed forecasting using wavelet transform and support vector machines optimized by genetic algorithm," *Renew. Energy*, vol. 62, pp. 592–597, Feb. 2014.
[29] J. Jin, B. Wang, M. Yu, and Q. Liu, "The short-term wind speed prediction based on HF-EMD and BP neural network model," in *Proc. 12th Conf. Ind. Electron. Appl.*, Jun. 2017, pp. 489–494.
[30] A. A. Abdoos, "A new intelligent method based on combination of VMD and ELM for short term wind power forecasting," *Neurocomputing*, vol. 203, pp. 111–120, Aug. 2016.
[31] A. Tascikaraoglu, B. M. Sanandaji, K. Poolla, and P. Varaiya, "Exploiting sparsity of interconnections in spatio-temporal wind speed forecasting using wavelet transform," *Appl. Energy*, vol. 165, pp. 735–747, Mar. 2016.
[32] S. Lahmiri, "Comparing variational and empirical mode decomposition in forecasting day-ahead energy prices," *IEEE Syst. J.*, vol. 11, no. 3, pp. 1907–1910, Sep. 2017.
[33] Y. Ren, P. N. Suganthan, and N. Srikanth, "A comparative study of empirical mode decomposition-based short-term wind speed forecasting methods," *IEEE Trans. Sustain. Energy*, vol. 6, no. 1, pp. 236–244, Jan. 2015.
[34] Z. Sun and M. Zhao, "Short-term wind power forecasting based on VMD decomposition, ConvLSTM networks and error analysis," *IEEE Access*, vol. 8, pp. 134422–134434, 2020.
[35] Y. Zhang, Y. Zhao, and S. Gao, "A novel hybrid model for wind speed prediction based on VMD and neural network considering atmospheric uncertainties," *IEEE Access*, vol. 7, pp. 60322–60332, 2019.
[36] Y. Chen and C. Yi, "Research on a new singularity-free controller for uncertain lorenz system," *IEEE Access*, vol. 7, pp. 136290–136298, 2019.
[37] M. Y. Yu, "Some chaotic aspects of the Lorenz-Stenflo equations," *Phys. Scripta*, vol. 82, no. 1, pp. 10–11, 1999.
[38] Z. J. Da, S. Mu, D. S. Ma, H. P. Yu, W. Hou, and Z. Q. Gong, "The theoretical study of the turning period in numerical weather prediction models based on the Lorenz equations," *Acta Phys. Sinica*, vol. 63, pp. 29201–29214, May 2014.
[39] Y. G. Zhang, Y. Zhao, G. F. Pan, and J. F. Zhang, "Wind speed interval prediction based on lorenz disturbance distribution," *IEEE Trans. Sustain. Energy*, vol. 11, no. 2, pp. 80–816, Apr. 2019.
[40] B. Z. Liu, J. H. Peng, *Nonlinear Dynamics*. Beijing, China: Higher Education Press, 2007.
[41] N. E. Huang, Z. Shen, S. R. Long, M. C. Wu, H. H. Shih, Q. Zheng, N.-C. Yen, C. C. Tung, and H. H. Liu, "The empirical mode decomposition and the Hilbert spectrum for nonlinear and non-stationary time series analysis," *Proc. Roy. Soc. London. Ser. A, Math., Phys. Eng. Sci.*, vol. 454, no. 1971, pp. 903–995, Mar. 1998.
[42] Z. Wu and N. E. Huang, "Ensemble empirical mode decomposition: A noise-assisted data analysis method," *Adv. Adapt. Data Anal.*, vol. 1, no. 1, pp. 1–41, Jan. 2009.
[43] N. Sarkar and B. B. Chaudhuri, "An efficient differential box-counting approach to compute fractal dimension of image," *IEEE Trans. Syst., Man, Cybern.*, vol. 24, no. 1, pp. 115–120, Jan. 1994.
[44] S. C. Wang, J. F. Zhang, F. Feng, X. Qian, L. Q. Jiang, J. L. Huang, B. B. Liu, J. Li, Y. S. Xia, and P. F. Feng, "Fractal analysis on artificial profiles and electroencephalography signals by roughness scaling extraction algorithm," *IEEE Access*, vol. 7, pp. 89265–89277, 2019.
[45] A. J. Hu, J. J. Sun, and L. Xiang, "Mode mixing in empirical mode decomposition," *J. Vibrat. Meas. Diagnosis*, vol. 31, no. 4, pp. 429–434, 2011.

JI JIN was born in 1993. He received the B.S. degree in automatization from the Wuhan University of Science and Technology, Wuhan, China, in 2015, where he is currently pursuing the M.S. and Ph.D. degrees in control science and engineering. His research topics include wind speed data preprocessing and prediction algorithms.

BIN WANG received the B.S. degree in electric automatization from China Three Gorges University, Yichang, China, in 1985, and the M.S. degree in power system and automatization from Sichuan University, Chengdu, China, in 1994, and the Ph.D. degree in electrical and engineering from Blaise Pascal University, Clermont-Ferrand, France, in 2003. He is currently working as a Professor with the Wuhan University of Science and Technology, Wuhan, China. His research interests include the analysis of power quality and harmonic control, intelligent detection technology and signal processing, and the operation and control for microgrid.

MIN YU received the B.S. degree in applied mathematics from Jianghan University, in 1997, and the M.S. degree in applied mathematics from Wuhan University, Wuhan, China, in 2005, and the Ph.D. degree in control science and engineering from the Wuhan University of Science and Technology, Wuhan, in 2018. She is currently working as a Teacher with the Wuhan University of Science and Technology. Her research interest includes the application of fractal and wind speed prediction.

JIANG LIU received the B.S. degree in power electronics and the M.S. and Ph.D. degrees in control theory and control engineering from the Huazhong University of Science and Technology, Wuhan, China, in 2013 and 2019, respectively. He currently holds a postdoctoral position at the Wuhan University of Science and Technology, Wuhan, China, where he is engaged in teaching and research in the field of power electronics and motion control. His current research interests include power electronics, electrical drives, and model predictive control.

WENBO WANG received the B.S., M.S., and Ph.D. degrees in applied mathematics from Wuhan University, Wuhan, China, in 2000, 2003, and 2006, respectively. He is currently a Full Professor with the Wuhan University of Science and Technology, Wuhan. His current research interests include multi-scale analysis theory, nonlinear signal processing, and image processing.